Geometry, Reduction Potential, and Reorganization Energy of the Binuclear Cu_A Site, Studied by Density Functional Theory

Mats H. M. Olsson and Ulf Ryde*

Contribution from the Department of Theoretical Chemistry, Lund University, Chemical Centre, P.O. Box 124, S-221 00 Lund, Sweden

Received February 5, 2001

Abstract: The dimeric Cu_A site found in cytochrome *c* oxidase and nitrous oxide reductase has been studied with the density functional B3LYP method. We have optimized the structure of the realistic $(Im)(S(CH_3)_2)$-$Cu(SCH_3)_2Cu(Im)(CH_3CONHCH_3)$ model in the fully reduced, mixed-valence, and fully oxidized states. The optimized structures are very similar to crystal structures of the protein, which shows that the protein does not strain the site significantly. Instead, inorganic model complexes of the protein site are strained by the macrocyclic connections between the ligand models. For the mixed-valence (Cu^I+Cu^{II}) state, two distinct equilibrium structures were found, one with a short Cu−Cu distance, 248 pm, similar to the protein structure, and one with a longer distance, 310 pm, similar to what is found in inorganic models. In the first state, the unpaired electron is delocalized over both copper ions, whereas in the latter, it is more localized to one of the ions. The two states are nearly degenerate. The potential energy surfaces for the Cu−Cu, $Cu-S_{Met}$, and Cu−O interactions are extremely flat. In fact, all three distances can be varied between 230 and 310 pm at an expense in energy of less than 8 kJ/mol, which explains the large variation observed in crystal structures for these interactions. Inclusion of solvation effects does not change this significantly. Therefore, we can conclude that a variation in these distances can change the reduction potential of the Cu_A site by at most 100 mV. The model complex has a reorganization energy of 43 kJ/mol, 20 kJ/mol lower than for a monomeric blue-copper site. This lowering is caused by the delocalization of the unpaired electron in the mixed-valence state.

Introduction

Cytochrome *c* oxidase (EC 1.9.3.1) is the terminal oxidase in both prokaryotic and eukaryotic cells and it is responsible for the generation of cellular energy via oxidative phosphorylation.[1] It couples the catalytic four-electron reduction of O_2 to water and transmembrane proton pumping, which can be used for ATP synthesis and long-range electron transfer. The active site is a heme a_3−Cu_B binuclear site, whereas a second heme *a* and an additional copper site, Cu_A, serve as electron-transfer intermediates between cytochrome *c* and the active site. Recently, the structure of cytochrome *c* oxidase was determined by crystallography.[2−4] This solved an old controversy regarding the geometry of the Cu_A site[5,6] by showing that it is a binuclear copper site, bridged by two cysteine thiolate groups. Each copper ion is also bound to a histidine group and a weaker axial ligand, a methionine sulfur for one copper and a backbone carbonyl group for the other. The Cu−Cu distance is extremely short, about 245 pm,[7] and it has been speculated that it represents a covalent bond.[8−10] A similar site is also found in nitrous oxide reductase[11] (EC 1.7.99.6), another terminal oxidase, which converts N_2O to N_2 in denitrifying bacteria. The structure of this protein was published last year.[12]

During electron transfer, the Cu_A site alternates between the fully reduced and the mixed-valence form (Cu^I+Cu^{II}). Interestingly, the unpaired electron in the mixed-valence form seems to be delocalized between the two copper ions. The Cu_A site has been thoroughly studied by various experimental methods.[8,13−28] Several theoretical investigations of the electronic

* Corresponding author. Fax: +46-46 222 45 43. E-mail: Ulf.Ryde@teokem.lu.se.

(1) Babcock, G. T.; Wikström, M. *Nature* **1992**, *356*, 301.
(2) Iwata, S.; Ostermeier, C.; Ludwig, B.; Michel, H. *Nature* **1995**, *376*, 660.
(3) Wilmanns, M.; Lappalainen, P.; Kelly, M.; Sauer-Erisson, E.; Saraste, M. *Proc. Natl. Acad. Sci. U.S.A.* **1995**, *92*, 11955.
(4) Tusihara, T.; Aoyama, H.; Yamashita, E.; Tomizaki, T.; Yamaguchi, H.; Shinwawa-Ithoh, K.; Nakashima, R.; Yaono, R.; Yoshikawa, S. *Science* **1995**, *269*, 1069.
(5) Malmström, B. G.; Aasa, R. *Eur. J. Biochem.* **1993**, *325*, 49.
(6) Beinert, H. *Eur. J. Biochem.* **1997**, *245*, 521.
(7) Blackburn, N. J.; de Vries, S.; Barr, M. E.; Houser, R. P.; Tolman, W. B.; Sanders, D.; Fee, J. A. *J. Am. Chem. Soc.* **1997**, *119*, 6135.
(8) Gamelin, D. R.; Randall, D. W.; Hay, M. T.; Houser, R. P.; Mulder, T. C.; Canters, G. W.; de Vries, S.; Tolman, W. B.; Li, Y.; Solomon, E. I. *J. Am. Chem. Soc.* **1998**, *120*, 5246.
(9) Blackburn, N.; Barr, M. E.; Woodruff, W. H.; van der Oost, J.; de Vries, S. *Biochemistry* **1994**, *33*, 10401.
(10) Wallace-Williams, S. E.; James, C. A.; de Vries, S.; Saraste, M.; Lappalainen, P.; van der Oost, J.; Fabian, M.; Palmer, G.; Woodruff, W. H. *J. Am. Chem. Soc.* **1996**, *118*, 3986.
(11) Kroneck, H.; Antholine, W. E.; Kastrau, D. H. W.; Buse, G.; Steffens, G. C. M.; Zumft, W. G. *FEBS Lett.* **1990**, *268*, 274.
(12) Brown, K.; Tegoni, M.; Prudencio, M.; Pereira, A. S.; Besson, S.; Moura, J. J.; Moura, I.; Cambillau, C. *Nat. Struct. Biol.* **2000**, *7*, 191.
(13) Andrew, C. R.; Franczkiewicx, R.; Czernuszewicz, R. S.; Lappalainen, P.; Saraste, M.; Sanders-Loehr, J. *J. Am. Chem. Soc.* **1996**, *118*, 10436.
(14) Bertini, I.; Bren, K. L.; Clemente, A.; Fee, J. A.; Gray, H. B.; Lucinat, C.; Malmström, B. G.; Richards, J. H.; Sanders, D.; Slutter, C. E. *J. Am. Chem. Soc.* **1996**, *118*, 11658.
(15) Brzezinski, P. *Biochemistry* **1996**, *7*, 5611.
(16) Dennison, C.; Berg, A.; de Vries, S.; Canters, G. W. *FEBS Lett.* **1996**, *394*, 340.
(17) Farrar, J. A.; Neese, F.; Lappalainen, P.; Kroneck, P. M. H.; Saraste, M.; Zumft, W. G.; Thomson, A. J. *J. Am. Chem. Soc.* **1996**, *118*, 11501.
(18) Immoos, C.; Hill, M. G.; Sanders, D.; Fee, J. A.; Slutter, C. E.; Richards, J. H.; Gray, H. B. *J. Biol. Inorg. Chem.* **1996**, *1*, 529.
(19) Karpefors, M.; Slutter, C. E.; Fee, J. A.; Aasa, R.; Källebring, B.; Larsson, S.; Vänngård, T. *Biophys. J.* **1996**, *71*, 2823.
(20) Neese, F.; Zumft, W. G.; Antoline, W. E.; Kroneck, P. M. H. *J. Am. Chem. Soc.* **1996**, *118*, 8692.
(21) Dennison, C.; Berg, A.; Canters, G. W. *Biochemistry* **1997**, *36*, 3262.

10.1021/ja010315u CCC: $20.00
Published on Web 07/20/2001

structure and spectrum of the Cu_A dimer have also appeared.[8,17,19,20,22,24,29,30]

The crystal structures of Cu_A from both native proteins, engineered sites in blue copper proteins or other oxidases, and inorganic model systems[2−4,7,12,17,31−34] show a conspicuous variation in some of the geometric parameters, cf. Table 1. In particular, the Cu−Cu distance varies between 220 and 302 pm, the axial Cu−S_{Met} bond length between 239 and 300 pm, and the axial Cu−O distance between 219 and 277 pm. Parts of this variation can be explained by the low resolution of the crystal structures, but the variation is so large that some of the differences must be real. For example, a model complex synthesized by Tolman and co-workers clearly has a longer Cu−Cu bond (293 pm) and shorter axial interactions than in the proteins (see Table 1).[34] Solomon and co-workers have studied the differences between this complex and the Cu_A site in cytochrome *c* oxidase in detail.[8] They suggest that the model system represents a strain-free Cu_A structure, and that the protein changes the electronic state and the properties of the site by enforcing longer distances to the axial ligands. This weaker ligation is compensated by the formation of a Cu−Cu bond, and these variations in the copper bond lengths should be used to fix the reduction potential.

This is similar to what has been suggested for the blue copper proteins.[35−39] However, we have argued strongly against any significant role of mechanical strain for the structure or properties of the blue-copper site.[40−43] Instead, we have shown that the large variation in the axial Cu−S_{Met} distance observed for these proteins can be explained by the flat potential surface of this interaction. In fact, the Cu−S_{Met} bond length can be varied over more than 80 pm at an energy cost of less than 7 kJ/mol. Therefore, it cannot have any significant influence on the structure or the reduction potential of the site.[42,43]

With this in mind, we here investigate the structure, reorganization energy, and reduction potential of the Cu_A site with the same theoretical methods as for the blue copper proteins.[40−42] Not too surprisingly, we find that the Cu_A site behaves similarly. The optimum structure of our realistic model in a vacuum is close to the geometry of the protein obtained by crystallography or extended X-ray absorption fine structure (EXAFS) measurements. The Cu−Cu, Cu−S_{Met}, and Cu−O bonds are flexible and therefore have small influence on the structure and reduction potential of the site. The results also allow us to calculate the reorganization energy for the site and compare it to that of the blue-copper site.

Methods and Details of Calculations

The Cu_A site in cytochrome *c* oxidase and nitrous oxide reductase consists of $HisMetCuCys_2CuHisGlu/Trp$, where the backbone carbonyl oxygen is the coordinating atom of the last amino acid. This site has been modeled by $(Im)(S(CH_3)_2)Cu(SCH_3)_2Cu(Im)(CH_3CONHCH_3)$, where Im denotes imidazole, that is, using ligand models that have been shown to give accurate results for the blue copper proteins.[40,44,45]

The geometries of four electronic states of the model complex were studied with the hybrid density functional method B3LYP as implemented in the quantum chemical software Turbomole.[46,47] The structures were optimized until the change in energy between two iterations was below 0.26 J/mole and the norm of the internal gradients was below 0.0053 pm or 0.0057° (these criteria are one magnitude stricter than default in Turbomole, and they have been used since the potential surface is very flexible for the bonds between the copper ions and the axial ligands). Several starting structures were tested to reduce the risk of being trapped in local minima. Only the structures with the lowest energy are reported. In all calculations, we have used for copper the double-ζ basis set of Schäfer et al.[48] (62111111/33111/311), enhanced with diffuse *p*, *d*, and *f* functions with exponents 0.174, 0.132, and 0.39 (called DZpdf). For the other atoms, the 6-31G* basis set was employed.[49] Only the pure five *d* and seven *f*-type functions were used. Experience have shown that geometries obtained with the B3LYP approach do not change much when the basis set is increased beyond this level.[40,44] Relative energies were obtained by single-point calculations on these structures also with the B3LYP method but with the larger 6-311+G(2d,2p) basis set[49] (for Cu, the DZpdf basis was extended by one set of *s*, *p*, and *f* functions with exponents 0.0155065, 0.046199, and 3.55, respectively). This improvement of the basis set did not change the energies by more than 3 kJ/mol.

Frequencies were calculated for the optimized structures using the Gaussian 98 program.[50] For Cu_A, a frequency calculation of the full models could not be performed in a reasonable time. Therefore, we instead used models without the axial ligands ($(Im)Cu(SCH_3)_2Cu(Im)$) but at the same geometry as the full models. Force constants for the various bonds, angles, and dihedrals in the complexes were estimated from the Hessian matrix using the algorithm suggested by Seminario.[51] It has the advantage of being fully invariant to the choice of internal coordinates. The force constants were used to calculate approximate contributions to the reorganization energy from the various internal distortions using a simple harmonic model.[41]

(22) Williams, K. R.; Gamelin, D. R.; LaCroix, L. B.; Houser, R. P.; Tolman, W. B.; Mulder, T. C.; de Vries, S.; Hedman, B.; Hodgson, K. O.; Solomon, E. I. *J. Am. Chem. Soc.* **1997**, *119*, 11501.
(23) Farrar, J. A.; Zumft, W. G.; Thomson, A. J. *Proc. Natl. Acad. Sci. U.S.A.* **1998**, *95*, 9891.
(24) Neese, F.; Kappl, R.; Hüttermann, J.; Zumft, W. G.; Kroneck, P. M. H. *J. Biol. Inorg. Chem.* **1998**, *3*, 53.
(25) Salgado, J.; Warmerdam, G.; Bubacco, L.; Canters, G. W. *Biochemistry* **1998**, *37*, 7378.
(26) Farver, O.; Lu, Y.; Ang, M. C.; Pecht, I. *Proc. Natl. Acad. Sci. U.S.A.* **1999**, *96*, 899.
(27) Kolczak, U.; Salgado, J.; Saraste, M.; Canters, G. W. *Biospectroscopy* **1999**, *5*, S19.
(28) Randall, D. W.; Gamelin, D. R.; LaCroix, L. B.; Solomon, E. I. *J. Biol. Inorg. Chem.* **2000**, *5*, 16.
(29) Farrar, J. A.; Grinter, R.; Neese, F.; Nelson, J.; Thompson, W. H. *J. Chem. Soc., Dalton Tran.* **1997**, 4083−4087.
(30) Larsson, S. *J. Biol. Inorg. Chem.* **2000**, *5*, 560.
(31) Williams, P. A.; Blackburn, N. J.; Sanders, D.; Bellamy, H.; Stura, E. A.; Fee, J. A.; McRee, D. A. *Nat. Struct. Biol.* **1999**, *6*, 509.
(32) Yoshikawa, S.; Shinzawa-Itoh, K.; Nakashima, R.; Yaono, R.; Yamashita, E.; Inoue, N.; Yao, M.; Fei, M. J.; Libeu, C. P.; Mizushima, T.; Yamaguchi, H.; Tomizaki, T.; Tsukihara, T. *Science* **1998**, *280*, 1723.
(33) Houser, R. P.; Halfen, J. A., Jr., V. G. Y.; Blackburn, N. J.; Tolman, W. B. *J. Am. Chem. Soc.* **1995**, *117*, 10745.
(34) Houser, R. P.; Young, V. G.; Tolman, W. B. *J. Am. Chem. Soc.* **1996**, *118*, 2101.
(35) da Silva, J. J. R. F.; Williams, R. J. P. *The Biological Chemistry of the Elements*; Clarendon: Oxford, 1991.
(36) Malmström, B. G. *Eur. J. Biochem.* **1994**, *223*, 207.
(37) Guckert, J. A.; Lowery, M. D.; Solomon, E. I. *J. Am. Chem. Soc.* **1995**, *117*, 2817.
(38) Wittung-Stafshede, P.; Hill, M. G.; Gomez, E.; Di Bilio, A. J.; Karlsson, B. G.; Leckner, J.; Winkler, J. R.; Gray, H. B.; Malmström, B. G. *J. Biol. Inorg. Chem.* **1998**, *3*, 367.
(39) Malmström, B. G.; Leckner, J. *Curr. Opin. Chem. Biol.* **1998**, *2*, 286.
(40) Ryde, U.; Olsson, M. H. M.; Pierloot, K.; Roos, B. O. *J. Mol. Biol.* **1996**, *261*, 586.
(41) Olsson, M. H. M.; Ryde, U.; Roos, B. O. *Protein Sci.* **1998**, *7*, 2659.
(42) Olsson, M. H. M.; Ryde, U.; Roos, B. O. *J. Biol. Inorg. Chem.* **1999**, *4*, 654.
(43) De Kerpel, J. O. A.; Ryde, U. *Proteins: Struct., Funct., Genet.* **1999**, *36*, 157.
(44) Ryde, U.; Olsson, M. H. M.; Roos, B. O.; Carlos, A. B. *Theor. Chim. Acta* **2001**, *105*, 452.
(45) De Kerpel, J. O. A.; Pierloot, K.; Ryde, U. *J. Phys. Chem. B* **1999**, *103*, 8375.
(46) Ahlrichs, R.; Bär, M.; Baron, H.-P.; Bauernschmitt, R.; Böcker, S.; Ehrig, M.; Eichkorn, K.; Elliott, S.; Haase, F.; Häser, M.; Horn, H.; Huber, C.; Kölmel, C.; Kollwitz, M.; Ochsenfeld, C.; Öhm, H.; Schäfer, A.; Schneider, U.; Treutler, O.; von Arnim, M.; Weigend, F.; Weis, P.; Weiss, H. *TURBOMOLE*, version 4.5; Universität Karlsruhe: Germany, 1997.
(47) Hertwig, R. H.; Koch, W. *Chem. Phys. Lett.* **1997**, *268*, 345.
(48) Schäfer, A.; Horn, H.; Ahlrichs, R. *J. Chem. Phys.* **1992**, *97*, 2571.
(49) Hehre, W. J.; Radom, L.; v. R. Schleyer, P.; Pople, J. A. *Ab initio Molecular Orbital Theory*; Wiley-Interscience: New York, 1986.

Table 1. Bond Lengths in Four Electronic States of the (Im)($S(CH_3)_2$)Cu($SCH_3)_2$Cu(Im)($CH_3CONHCH_3$) Model Compared to Experimental Data for the Cu_A Site in Crystal Structure and Model Compounds

oxidation state	Cu−Cu	Cu−S_{Cys}	Cu−N_{His}	Cu−S_{Met}	Cu−O
I+I	257	233−247	207−211	240	250
I+I; X-ray[12]	247	226−231	198−207	247	260
I+I; EXAFS[7]	251−252	231−238	195−197	−	−
I+II; X-ray[2−4,17,31,32]	220−258	217−240	185−211	239−272	219−277
I+II; EXAFS[7,59]	243−246	229−233	195−203	−	−
I+II σ^*	248	231−235	202−209	245	220
I+II π	310	227−236	203−210	242	219
I+II; model[34]	290−293	223−230	209−213[a]		
II+II	342	228−234	202−203	242	202
I+II; model[33]	334	233	206[a]		210−226[a]

[a] Both the N_{His} groups and the axial ligands are amine nitrogen atoms in the models.

Furthermore, we have investigated the effect of variations in the Cu−Cu, Cu−S_{Met}, and Cu−O bond lengths on the potential energy and reduction potential. The potential energy surfaces were obtained by constraining these distances to at least five values between 230 and 310 pm, while fully relaxing the rest of the geometry.

We have also studied how the reduction potential varies as a function of these three distances. When calculating reduction potentials, solvation effects are almost as important as electronic effects. Therefore, the solvation energy of the copper complexes was estimated by the polarized continuum method (PCM).[52] In this method, the molecule is placed in a cavity formed by overlapping atom-centered spheres surrounded by a dielectric medium. The induced polarization of the surroundings is represented as point charges distributed on the surface of the cavity, and the field from these charges in its turn affects the wave function. We have used the conductor PCM method, CPCM,[53] as implemented in the Gaussian 98 software.[50] It involves three contributions to the free energy of the solvation in addition to the described electrostatic interaction between the solute and the solvent, viz. the energy of forming a cavity in the solvent, the dispersion solute−solvent energy, and the exchange solute−solvent energy, respectively.[54−56] These terms, which affect only the solute energy and not its wave function have not been included in the reported energies for reasons discussed before.[42]

The radii of the atomic spheres were obtained according to the united-atom model for Hartree−Fock (UAHF) strategy, where the size of the radii depends on the hybridization and substituents on each of the atoms. Hydrogen atoms are included in the radius of the heavier atoms to make the cavity surface smoother. This approach has been shown to give excellent agreement with experiments,[57] and it is the default procedure in Gaussian 98. To get a better description of the cavity surface and charges induced by the solute, a smaller than default area of each surface element has been used (TSARE = 0.4 Å^2). The dielectric constant of water (78.39) was used in all calculations, to give an upper limit of the solvation effects (see below). The reduction potentials were calculated as the direct difference between the CPCM (single-point) energies of the reduced and oxidized states in their respective optimized vacuum geometries.[42]

According to the semiclassical Marcus theory,[58] the rate of electron transfer is given by:

$$k_{ET} = \frac{2\pi}{\hbar}\frac{H_{DA}^2}{\sqrt{4\pi\lambda RT}}\exp\left(-\frac{(\Delta G^\circ + \lambda)^2}{4\lambda RT}\right) \quad (1)$$

Here, H_{DA} is the electronic coupling matrix element, which depends on the overlap of the wave functions of the two states involved in the reaction, λ is the reorganization energy, the energy associated with relaxing the geometry of the system after electron transfer, and ΔG° is the free energy change of the reaction, that is, the reduction potential.

For convenience, the reorganization energy is usually divided into two parts: inner-sphere, λ_i, and outer-sphere reorganization energy, λ_o, depending on which atoms are relaxed. For a metal-containing protein, the inner-sphere reorganization energy is associated with the structural change of the first coordination sphere of the metal, whereas the outer-sphere reorganization energy involves structural changes of the remaining protein as well as those of the solvent. In general, the reorganization energy is defined as the energy needed to distort the nuclear configuration for the initial state to that of the final state on the energy surface of the initial state. Thus, λ_{ox} can be calculated as the difference between the energy of the oxidized complex at the optimal geometry of the reduced complex and of the oxidized complex. Likewise, λ_{red}, is the energy difference of the reduced complex at the optimal oxidized geometry and the optimal reduced geometry. The total inner-sphere reorganization energy of a self-exchange electron-transfer reaction is the sum of these two reorganization energies for the site. In variance to the outer-sphere reorganization energy, the inner-sphere reorganization energy is independent of the actual geometry of the docking complex between donor and acceptor sites and can therefore be studied for isolated complexes.[41]

All calculations were run on IBM SP2, SGI Origin 2000, or Octane workstations.

Results and Discussion

The σ-Bonded Mixed-Valence State of Cu_A. The experimentally most studied state of Cu_A is the mixed-valence state ($Cu^I + Cu^{II}$). Several techniques have been used to probe the structure of the Cu_A site. Protein crystallography has revealed an unusually short Cu−Cu distance, (220−258 pm), and a broad distribution of Cu−S_{Cys} (217−240 pm), and Cu−N_{His} distances (185−211 pm).[2−4,7,17,31,32] Including engineered sites in the comparison increases the range of measured distances further. Our optimized structure of (Im)($S(CH_3)_2$)Cu($SCH_3)_2$Cu(Im)-($CH_3CONHCH_3$) in the mixed-valence state is similar to available experimental structure data. As can be seen in Figure 1 and Table 1, all of the theoretical Cu−ligand bond lengths are within the range of the crystal structures.

EXAFS studies normally give more accurate metal−ligand distances than protein crystallography. The mixed-valence form of the Cu_A site from bovine and two bacterial cytochrome *c*

(50) Frisch, M. J.; Trucks, G. W.; Schlegel, H. B.; Scuseria, G. E.; Robb, M. A.; Cheeseman, J. R.; Zakrzewski, V. G.; Montgomery, J. A.; Stratmann, R. E.; Burant, J. C.; Dapprich, S.; Millam, J. M.; Daniels, A. D.; Kudin, K. N.; Strain, M. C.; Farkas, O.; Tomasi, J.; Barone, V.; Cossi, M.; Cammi, R.; Mennucci, B.; Pomelli, C.; Adamo, C.; Clifford, S.; Ochterski, J.; Petersson, G. A.; Ayala, P. Y.; Cui, Q.; Morokuma, K.; Malick, D. K.; Rabuck, A. D.; Raghavachari, K.; Foresman, J. B.; Cioslowski, J.; Ortiz, J. V.; Stefanov, B. B.; Liu, G.; Liashenko, A.; Piskorz, P.; Komaromi, I.; Gomperts, R.; Martin, R. L.; Fox, D. J.; Keith, T.; Al-Laham, M. A.; Peng, C. Y.; Nanayakkara, A.; Gonzalez, C.; Challacombe, M.; Gill, P. M. W.; Johnson, B.; Chen, W.; Wong, M. W.; Andres, J. L.; Head-Gordon, M.; Replogle, E. S.; Pople, J. A. *Gaussian 98, revision A.5*; Gaussian, Inc.: Pittsburgh, PA, 1998.

(51) Seminario, J. M. *Int. J. Quantum Chem.: Quantum Chem., Symp.* **1996**, *30*, 59.

(52) Tomasi, J.; Persico, M. *Chem. Rev.* **1994**, *94*, 2027.

(53) Barone, V.; Cossi, M. *J. Phys. Chem. A* **1998**, *102*, 1995.

(54) Periotti, R. A. *Chem. Rev.* **1976**, *76*, 717.

(55) Floris, F. M.; Tomasi, J. *J. Comput. Chem.* **1989**, *10*, 616.

(56) Floris, F. M.; Tomasi, J.; Pascual-Ahuir, J. L. *J. Comput. Chem.* **1991**, *12*, 784.

(57) Barone, V.; Cossi, M.; Tomasi, J. *J. Chem. Phys.* **1997**, *107*, 3210.

(58) Marcus, R. A.; Sutin, N. *Biochim. Biophys. Acta* **1985**, *811*, 265.

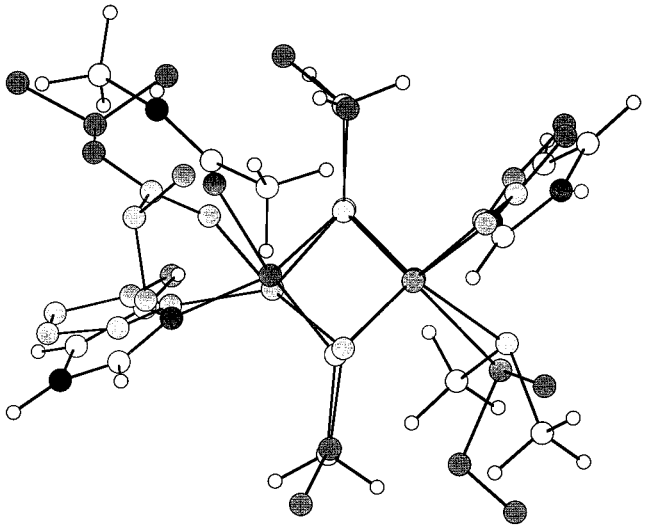

Figure 1. Optimized structure of the σ^* mixed-valence $(Im)(S(CH_3)_2)Cu(SCH_3)_2Cu(Im)(CH_3CONHCH_3)$ complex compared to the crystal structure of the Cu_A site in cytochrome *c* oxidase (shaded and without any hydrogen atoms).[32]

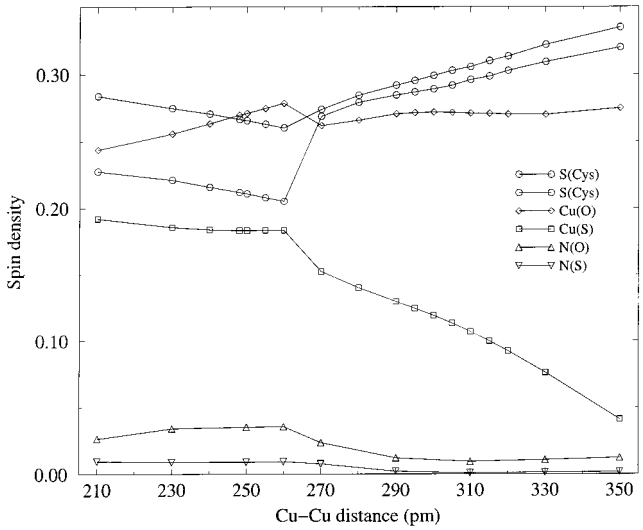

Figure 2. Spin density of the mixed-valence $(Im)(S(CH_3)_2)Cu(SCH_3)_2Cu(Im)(CH_3CONHCH_3)$ model as a function of the Cu−Cu distance.

oxidases has been studied with this method.[7,59] The observed Cu−Cu distances (243−246 pm) are slightly shorter than our estimate (248 pm). Considering the flat Cu−Cu potential (see below), the difference is very small in energy terms (less than 1 kJ/mol). The experimental $Cu-S_{Cys}$ distances, 229−233 pm, are close to our calculated distances (231−235 pm). However, somewhat larger discrepancies are found for the $Cu-N_{His}$ distance. The two $Cu-N_{His}$ distances in our optimized model are 202 and 209 pm, whereas the EXAFS experiment gives 195−203 pm. The difference is slightly larger than what is normally found for metal bonds to histidine ligands optimized with the B3LYP method (4−5 pm),[60] but our calculations on the Tolman model complex below indicate that this is a typical error for this type of complexes.

Our optimized S−Cu−S angles, 114−116°, agree excellently with what is observed in crystal structures (111−119°) and in EXAFS experiments (115°).[2−4,7,31,32] Even the distances to the axial ligands are within the experimentally observed range: 245 pm for the methionine ligand and 220 pm for the backbone carbonyl group, compared to 241−272 and 219−277 pm, respectively, in crystal structures (they are not observed in EXAFS experiments). All of these results clearly show that the protein does not induce any larger changes of the Cu_A geometry.

The π-Bonded Mixed-Valence State of Cu_A. It has been noted that some inorganic models of the Cu_A site have an appreciably longer Cu−Cu distance (around 290 pm).[34] It has been suggested that this is the natural (unstrained) state of Cu_A and that the short bond in the protein can be attributed to protein strain.[8] More precisely, it has been suggested that the protein enforces long $Cu-S_{Met}$ and Cu−O distances onto the site (the distances to the axial ligands in the model are very short, 212 pm). The reduction of charge donation to the copper ions is compensated by shortening the other copper−ligand distances, including the Cu−Cu distance. This could lead to formation of a Cu−Cu bond and a change in electronic ground state in the protein. Electronic structure calculations of the Cu_A site in the protein have shown that the singly occupied orbital is σ^* with respect to the Cu−Cu axis (an orbital of B_{3u} symmetry in an idealized D_{2h} point group), whereas it is π bonding in the inorganic model complex (B_{2u}).[8,17,22,28]

We have also been able to optimize the structure of the π-bonded electronic state. In a vacuum, it is characterized by a Cu−Cu distance of 310 pm and a slightly larger variation in the $Cu-S_{Cys}$ distances (227−236 pm). The other geometric parameters are quite similar to the σ-bonded structure. Compared to the Tolman structure[34] (cf. Table 1), our $Cu-S_{Cys}$ distances are similar, whereas the calculated Cu−Cu distance is 13 pm too long. Again, this is most likely an effect of the flat potential of this interaction, combined with the differences in the model systems (the model complex has four equivalent Cu−N bonds at 211−212 pm from the copper ions). A prominent difference between the two mixed-valence structures is the S−Cu−S angles. As was mentioned above, they are around 115° in the σ-bonded structure, but only 95−97° in the other structure. In the Tolman model, they are 100°.

Interestingly, the σ^*- and the π-bonded structures are almost degenerate in energy; in our calculations, the π-bonded structure is 2 kJ/mol lower in energy than the σ-bonded one, but this difference is well within the error limit of the B3LYP method. This is in accordance with paramagnetic nuclear magnetic resonance (NMR) experiments, which have been suggested to show that the excited π state is thermally accessible at room temperature, with an energy difference of 4 kJ/mol.[25,27]

Spin Populations. The two electronic states of the mixed-valence Cu_A complex differ in the localization of the unpaired electron: in the σ^* state (found in the protein) the electron is delocalized over the entire CuS_2Cu system, whereas in the π state, the electron moves to Cu_S (the copper ion coordinated to the methionine ligand) and the two sulfur atoms. The remaining spin density resides on the other copper ion, 11%. This is succinctly shown in Figure 2 where the spin population of the various atoms are shown as a function of the Cu−Cu distance. The discontinuity around 270 pm represents the change in the electronic state. It is also notable that the spin population on the imidazole ligands depends strongly on the electronic ground state; when going from the σ^* to the π state, it decreases from 5 to 1%. In fact, the identification of the ground state as σ^* was based on the high observed spin population on the imidazole groups.[20]

The spin population at the equilibrium structures can be compared to experimental results obtained by paramagnetic

(59) Henkel, G.; Müller, A.; Weissgräber, S.; Buse, G.; Soulimane, T.; Steffens, G. C. M.; Nolting, H.-F. *Angew. Chem., Int. Ed. Engl.* **1995**, *34*, 1489.

(60) Sigfridsson, E.; Olsson, M. H. M.; Ryde, U. *J. Phys. Chem., B* **2001**, *105*, 5546−5552.

Table 2. Spin Density in the Mixed-Valence States of the $(Im)(S(CH_3)_2)Cu(SCH_3)_2Cu(Im)(CH_3CONHCH_3)$ Model

	Cu_S	Cu_O	S_1	S_2	S_{Met}	O	Im
σ^*	18	27	27	21	3	0	5
π	11	27	31	30	0	0	1
experiments[20,24]	15−36	15−36	16−24	16−24			3−5

NMR, electron paramagnetic resonance (EPR), and electron−nuclear double resonance (ENDOR) spectroscopy as is done in Table 2. EPR measurements have indicated that the spin density on the copper ions is 15−20%, whereas the ENDOR estimates are slightly higher (20−30%).[20,24] Our result is intermediate: 18−27%. Similarly, NMR experiments have indicated a spin population of ∼20% on each thiolate bridge,[25,27] whereas ENDOR spectroscopy indicates that the spin density on each thiolate group is 16−24% and the density on the histidine ligands is 3−5%. Again, this is close to our results: 21−27 and 5%, respectively. Moreover, the spin populations on the two imidazole groups are not equivalent, they are 1 and 4% for our model. This is in agreement with ENDOR and NMR measurements on some proteins.[8,25,61] However, NMR results on other proteins indicate a more equal distribution.[27] This reflects that the relative populations on the histidine ligands depend on the structure of the complex, for example the bond lengths to the axial ligands.[27] Thus, our calculations reproduce experimental spin densities well, increasing the credibility of our results.

Interestingly, our calculated spin densities are not identical for the two copper ions even in the σ^* state. As can be seen in Table 2, the spin density on Cu_S is slightly lower than that on Cu_O (18 and 27%, respectively). This is quite natural since we have not enforced any symmetry onto the site and the axial ligands are different and bind at closer distances than in most crystal structures. In fact, our calculations show that the spin density changes quite strongly for limited changes in the structure. This is in accordance with the experimental observation that a mutant of cytochrome *c* oxidase[62] has a valence-trapped state and that a partly delocalized site has been observed for an engineered site in quinol oxidase.[63] Thus, the electronic state is very flexible, and it is likely that the electric field from nearby dipoles in the surrounding protein can influence the spin distribution.

The Fully Reduced State. The optimized geometry of the fully reduced Cu_A model is shown in Table 1 and Figure 3. The recent crystal structure of nitrous oxide reductase is in this state,[12] and there are also EXAFS data available for the reduced Cu_A site in cytochrome *c* oxidase.[7] All calculated distances are reasonably close to experimental data and often more similar to the EXAFS data than to the rather crude crystal structure (2.4 Å resolution). The distances between the copper ions and the strong ligands seem to be slightly too long (as usual), whereas those to the axial ligands are 7−10 pm too short. Considering the small force constant of the latter bonds (see below), that discrepancy is negligible in energy terms.

Interestingly, our optimized model complexes reproduce well the *change* in structure upon reduction. The average $Cu-S_{Cys}$, Cu−N, and Cu−Cu distances in our calculations increase by 6, 3, and 9 pm respectively, which is in excellent agreement with EXAFS data, 4, 1, and 8 pm, respectively. Moreover, the S−Cu−S angles remain at 111−117° when the site is reduced. Again, this agrees with EXAFS experiments, which give a S−Cu−S angle of 115° for both oxidation states. Evidently, the CuS_2Cu core expands, while the overall structure is retained. Thus, we see that even if there are clear discrepancies between the experimental and theoretical results, the deviations are systematic, and consequently, the change upon reduction is accurately estimated. Therefore, our calculated reorganization energies can be expected to be quite accurate.

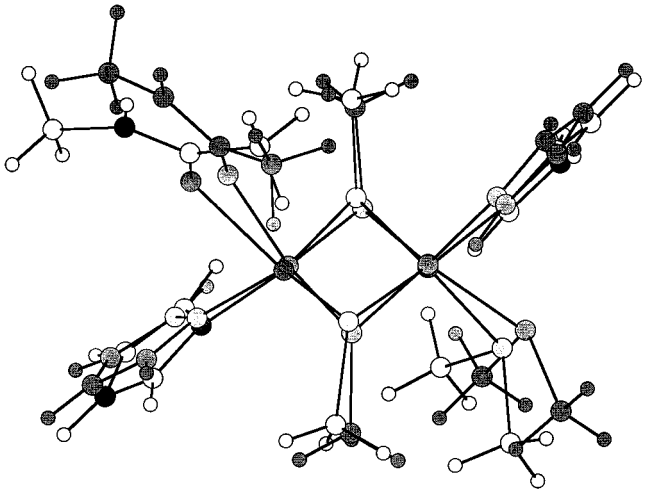

Figure 3. Structure of fully reduced $(Im)(S(CH_3)_2)Cu(SCH_3)_2Cu(Im)(CH_3CONHCH_3)$ model compared to the σ^* mixed-valence structure (shaded).

Table 3. Reorganization Energies (kJ/mol) for the Various Transitions of the $(Im)(S(CH_3)_2)Cu(SCH_3)_2Cu(Im)(CH_3CONHCH_3)$ Model[a]

states		reorganization energy		
reduced	oxidized	λ_i	λ_{red}	λ_{ox}
I+I	I+II σ^*	43.4	16.4	27.0
I+I	I+II π	69.0	40.4	28.5
I+II σ^*	II+II	133.9	46.5	87.5
I+II π	II+II	90.3	47.7	42.6
I	II	61.5	32.7	28.8

[a] Results for the plastocyanin model $Cu(Im)_2(SCH_3)(S(CH_3)_2)$ are included for comparison.[32]

In Table 3, self-exchange inner-sphere reorganization energies for our Cu_A model are reported. The reorganization energy for the electron transfer between the σ-bonded mixed-valence state and the fully reduced state is 43 kJ/mol. Experimental estimates of the total reorganization energy of the Cu_A site have in general been quite low, 15−50 kJ/mol.[15,26,64] However, recent accurate experiments indicate that the reorganization energy is appreciably larger, around 80 kJ/mol.[65] If we assume that the outer-sphere reorganization energy of cytochrome *c* oxidase is of the same magnitude as for plastocyanin (around 40 kJ/mol[66]), our calculated reorganization energy for Cu_A agrees with experiments.

Solomon and co-workers have estimated the inner-sphere reorganization energy of the Cu_A site by an excited-state distortion analysis of the resonance Raman enhancement profile to be about 24 kJ/mol.[8] However, as was discussed in our article

(61) Gurbiel, R. J.; Fann, Y. C.; Surerus, K. K.; Werst, M. M.; Musser, S. M.; Doan, P. E.; Chan, S. I.; Fee, J. A.; Hoffman, B. M. *J. Am. Chem. Soc.* **1993**, *115*, 10888.

(62) Farrar, J. A.; Lappalainen, P.; Zumft, W. G.; Saraste, M.; Thomson, A. J. *Eur. J. Biochem.* **1995**, *232*, 303.

(63) Kelly, M.; Lappalainen, P.; Talbo, G.; Halitia, T.; van der Oost, J.; Saraste, M. *J. Biol. Chem.* **1993**, *268*, 16781.

(64) Ramirez, B. E.; Malmström, B. G.; Winkler, R. J.; Gray, H. B. *Proc. Natl. Acad. Sci. U.S.A.* **1995**, *92*, 11949.

(65) Hoke, K. R.; Kiser, C. N.; di Bilio, A. J.; Winkler, R. J.; Richards, J. H.; Gray, H. B. *J. Inorg. Biochem.* **1999**, *74*, 165.

(66) Soriano, G. M.; Cramer, W. A.; Krishtalik, L. I. *Biophys. J.* **1997**, *73*, 3265.

Table 4. Contributions to the Reorganization Energies from Bonds to Copper in Blue-Copper and Cu_A Models[a]

	$Cu(Im)_2(SCH_3)(S(CH_3)_2)^{0/+}$				$(Im)Cu(SCH_3)_2Cu(Im)$			
bond	Δr	k^{red}	k^{ox}	λ_i	Δr	k^{red}	k^{ox}	λ_i
$Cu-S_{Cys}$	13.6	0.0194	0.0374	10.5	6.0	0.0116	0.0195	1.1
					0.4	0.0158	0.0223	0.1
					7.7	0.0119	0.0197	1.9
					12.0	0.0074	0.0155	3.3
$Cu-N_{His}$	10.2	0.0060	0.0225	3.0	4.5	0.0129	0.0249	0.8
	9.9	0.0074	0.0226	3.0	1.7	0.0101	0.0157	0.1
Cu−Cu					8.6	0.0074	0.0110	1.4

[a] The analysis is based on a force-constant analysis of the corresponding Hessian matrixes. Δr is the change in the bond length (pm), k^{red} and k^{ox} are the force constants of the reduced and the oxidized sites (kJ/mol/pm^2), and λ_i is the contribution to the inner-sphere reorganization energy (kJ/mol) calculated from these data.

about reorganization energy in the blue copper proteins,[41] such an energy applies to a *charge-transfer excitation* rather than to a full transfer of an electron. Therefore, it is not very surprising that their estimate is about half as large as ours.

It is instructive to compare the reorganization energy of Cu_A to that obtained for the blue copper proteins, for example 62 kJ/mol for plastocyanin.[41] Thus, the dimeric Cu_A site has ~20 kJ/mol lower reorganization energy than the monomeric blue-copper site. This is not unexpected; already 6 years ago, Larsson and co-workers suggested that the reorganization energy of the dimer should be half of that of the monomer.[30,67] The reason for this is that the unpaired electron in the dimer is delocalized over twice as many bonds as in the monomer, reducing the bond order by a factor of 2. The bond order determines the strength of the bond, and therefore the bond-length change upon reduction should be halved. The reorganization energy is approximately proportional to the square of the change in the bond lengths, but since there are twice as many bonds in the dimer as in the monomer, the reorganization energy should be reduced by a factor of 2.[30,67]

However, the dominant contribution to the reorganization energy in the blue copper proteins comes from the $Cu-S_{Cys}$ interaction,[41] and there are four such bonds in the Cu_A site, but only one in the blue copper proteins. Therefore, the $Cu-S_{Cys}$ bond should give the same contribution to the reorganization energy in the two sites. Yet, also the force constant of the Cu−ligand interactions decreases with the bond order. For example, it has been noted that vibrational energies of the copper site are appreciably lower for Cu_A than for the blue copper proteins, 100−350 cm^{-1} compared to 250−500 cm^{-1}.[8] Therefore, the inner-sphere reorganization energy of the Cu_A site can be expected to be lower than that of the blue copper proteins.

From our optimized bond lengths, collected in Table 4, it can be seen that the change in the bond lengths is really approximately halved. Upon reduction, the $Cu-S_{Cys}$ and $Cu-N_{His}$ distances change by 14 and 10 pm, respectively, on average in the plastocyanin model, but only 6 and 3 pm, respectively, for the Cu_A model. Still, the reorganization energy is only reduced by 33%, so that the angles and force constants are also important for the reorganization energy.[41] Therefore, we have calculated the corresponding force constants (also in Table 4). For the $Cu-S_{Cys}$ bonds, they decrease by 40−50%, whereas for the terminal $Cu-N_{His}$ bonds, they are almost unchanged and actually increase in the reduced state. However, since the changes in the bond lengths are strongly reduced for the Cu_A site, the total reorganization energy is reduced for both bonds, from 10 to 6 kJ/mol for the $Cu-S_{Cys}$ bonds and from 6 to 1 kJ/mol for the $Cu-N_{His}$ bonds.

The Cu−Cu interaction, which is only present in the Cu_A site, does not change the situation significantly; due to its small force constant, it contributes by only 1 kJ/mol to the total reorganization energy. However, the axial ligands also give a significant contribution to the reorganization energy. The $Cu-S_{Met}$ bond in the blue-copper model contributes by 7 kJ/mol to λ_i, whereas its contribution in the Cu_A site is negligible because of its small change (4 pm). On the other hand, the Cu−O bond in the Cu_A site (which is not present in our blue-copper model) changes by the same amount as the $Cu-S_{Met}$ bond in the blue-copper model (30 pm) and can therefore be predicted to give a similar contribution to λ_i.

Together, the bond lengths contribute to less than half of the reorganization energy. The rest comes from distortions of the angles and torsions. However, these the changes are so large that the harmonic approximation breaks down (in particular for the blue-copper model). Yet, it is clear that the total effect is smaller in the Cu_A model than in the blue-copper model. For example, the two $S_{Cys}-Cu-N_{His}$ angles in the blue-copper model change on average by 15°, giving a total λ_i of 25 kJ/mol, whereas the four angles in Cu_A change by 6°, on average, giving a total λ_i of only 8 kJ/mol. Besides this angle, only the $Cu-S_{Cys}-C$ angles give contributions larger than 1 kJ/mol in the Cu_A models, summing up to 7 kJ/mol (1 kJ/mol in the blue-copper site), whereas also the $Cu-N-C$, $Cu-S_{Met}-C$, $N-Cu-S_{Met}$, $C-S_{Met}-C$, and $N-Cu-N$ angles are important in the blue-copper models (42, 7, 6, 1, and 1 kJ/mol, respectively).

We have also calculated the reorganization energy for the transition between the fully reduced state and the π-bonded mixed-valence state. It is appreciably larger, 69 kJ/mol. From the data in Table 3, it is clear that the entire difference can be traced back to λ_{red}; λ_{ox} for the two processes are nearly the same. The most conspicuous difference in geometry between the σ^* and π states is the Cu−Cu distance. In the σ^* state, it is quite similar to the one in the fully reduced structure structure, whereas it is appreciably (53 pm) longer in the π state. From the Cu−Cu potential energy curve in Figure 4, we can see that this increase corresponds to 9 out of the 25 kJ/mol difference in reorganization energy. The remaining part is probably due to the change in the angles of the CuS_2Cu core resulting from the dilation in the π state. Contributions from the $Cu-S_{Met}$ and O distances are probably negligible due to their flat potential energy surfaces and small changes in distances (see below). The large reorganization energy for this transition explains why it is favorable for cytochrome *c* oxidase to have Cu_A in the σ^* state rather than the π state although the two states have almost the same energy.

Potential Energy Surfaces of the Cu−Cu, Cu−S_{Met}, and Cu−O Bonds. Since the electronic structure for the mixed-valence form of the $(Im)(S(CH_3)_2)Cu(SCH_3)_2Cu(Im)(CH_3CONHCH_3)$ complex is very flexible, it is not surprising to find that the potential surface for the Cu−Cu interaction is extremely flat. As can be seen in Figure 4, the barrier between the two electronic states (σ^* and π) is less than 5 kJ/mol, and the Cu−Cu distance can vary over 100 pm (240−340 pm) at a cost of less than 5 kJ/mol. This small variation in energy shows that the Cu−Cu interaction is extremely flexible and therefore may easily be affected by interactions with the surrounding protein. This explains the large variation in this bond length observed in protein crystal structures (220−258 pm[2−4,17,31,32]), and it also explains why some model complexes have longer Cu−Cu distances (up to 302 pm[17]).

(67) Larsson, S.; Källebring, B.; Wittung, P.; Malmström, B. G. *Proc. Natl. Acad. Sci. U.S.A.* **1995**, *92*, 7167.

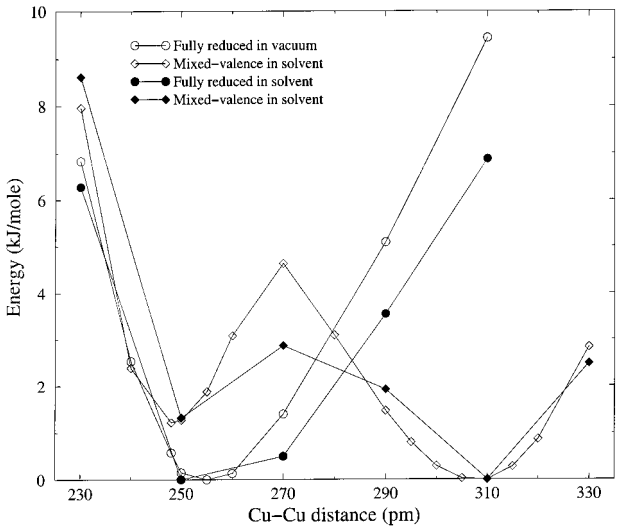

Figure 4. Potential energy surface of the Cu−Cu interaction in a vacuum and water for the mixed-valence and the fully reduced states.

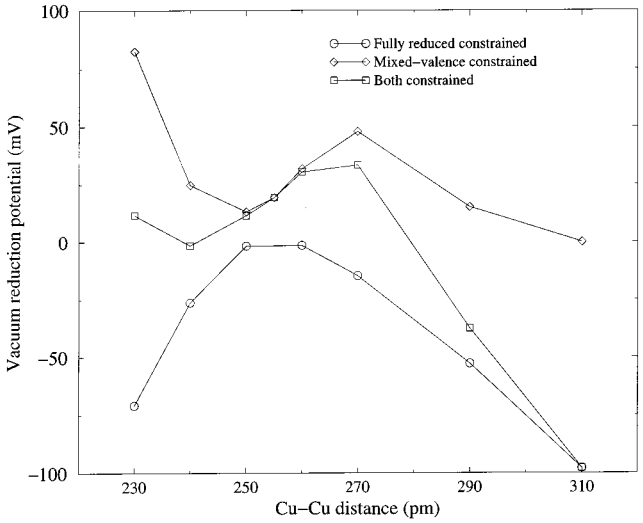

Figure 5. Calculated reduction potential for the Cu_A model between the mixed-valence and the fully reduced states as a function of constraints in the Cu−Cu bond length, calculated in a vacuum. The energy scale has been selected so that the unconstrained case has a reduction potential of 0 mV for all curves.

For the fully reduced state, things are very similar, except that there is only a single equilibrium structure. Thus, as can also be seen in Figure 4, the Cu−Cu distance can vary between 240 and 290 pm at a cost of less than 5 kJ/mol.

Recently, it has been suggested that the proteins fix the reduction potential of the Cu_A site by straining the Cu−Cu, Cu−S_{Met}, and Cu−O distances.[8,17] We test this suggestion by calculating how much the reduction potential can be altered by realistic constraints in these distances, starting with the Cu−Cu interaction. The reduction potential is simply the energy difference between the reduced and mixed-valence complexes at their optimum geometries. However, if the protein constrains the Cu−Cu distance, the energy of the two complexes will change according to the potential curves in Figure 4. The reduction potential can still be calculated as the difference in energy of the reduced and oxidized states, but now at non-optimal, constrained, geometries. Therefore, we must have a hypothesis about which state is constrained and to what extent (this is not specified in the original suggestion).[8] We have tested three resonable limiting cases, viz. that only the reduced state is constrained, that only the mixed-valence is constrained, or that both states are constrained to the same Cu−Cu distance.[42]

In Figure 5, the variations of the reduction potential for these three cases are shown. As expected, the reduction potential decreases if the reduced state is constrained (it is destabilized), it increases if the mixed-valence state is constrained, whereas it can both increase and decrease if both states are constrained. However, it is clear from the curves that constraints in the Cu−Cu distance can only have a limited effect on reduction potential, less than 100 mV in the range 230−310 pm. In particular, it can be seen that the reduction potential of the σ^* state is only 10 mV higher than that of the π-bonded state. Thus, the protein does not gain much in the reduction potential from stabilizing the σ^* state—the important effect comes instead from the reorganization energy, as we saw above.

All of these calculations were performed in a vacuum. However, for reduction potentials, solvation effects are as important as electronic effects. Therefore, we have also performed the same calculations in water solution. The dielectric constant of a protein has been much discussed, but it is usually assumed to be 2−16.[68−70] Therefore, our two calculations at dielectric constants of 1 (vacuum) and 78 (water), should include all realistic variations in any protein. Naturally, such a continuum approach does not take any account of the detailed structure of the proteins. However, we are only interested in how the reduction potentials change as an effect of constraints in the distance between the copper ions and their axial ligands, and these relative reduction potentials can be expected to be quite insensitive to details in the surroundings.

The potential curves for the Cu−Cu distance in the reduced and mixed-valence Cu_A model in water solution are also shown in Figure 4. It can be seen that they do not differ by more than 2 kJ/mol from the vacuum curves anywhere. The largest difference is that the barrier between the two electronic states of the mixed-valence complex is lowered to less than 3 kJ/mol. Figure 6 shows the reduction potential as a function of the Cu−Cu distance in water solution. A comparison to the corresponding vacuum curves in Figure 5 confirms that it does not depend much on the solvent. The only significant difference is seen at the largest distances, where the change in the reduction potential in water is less than in a vacuum (−75 compared to −100 mV). Of course, this does not change the general conclusion that constraints in the Cu−Cu distance cannot alter the reduction potential significantly. For the change in electronic state of the mixed-valence complex, the effect is still only ∼10 mV.

It has frequently been suggested that there is a Cu−Cu bond in the σ^* state.[8,9,22,10,28] However, the remarkable flexibility of the Cu−Cu bond in Figure 4, shows that no energy is gained by simply shortening the Cu−Cu distance. Thus, if there is any bond, it is not reflected in the energies. Similarly, the force-constant analysis gives no indication of a Cu−Cu bond. According to Seminario, for two atoms involved in a bond, the 3*3 submatrix of the Hessian involving these two atoms should have only negative eigenvalues (indicating that the molecule will restore a perturbation in this bond).[51] For our Cu_A models, such an analysis gives two positive eigenvalues both in the reduced and the σ^* mixed-valence states. Thus, the Cu−Cu interaction is not stable. Finally, it can be noted that the Mulliken overlap population in the σ^* mixed-valence state between the two copper ions (0.05−0.07 *e*) is 4 times smaller than that of the Cu−S_{Cys} and Cu−N_{His} bonds (0.15−0.21 *e*), and even half as large as that of the axial Cu−O and Cu−S_{Met} bonds (0.10−

(68) Sharp, K. A. *Annu. Rev. Biophys. Biophys. Chem.* **1990**, *19*, 301.
(69) Rodgers, K. K.; Sligar, S. G. *J. Am. Chem. Soc.* **1991**, *113*, 9419.
(70) Honig, B. *Science* **1995**, *268*, 1144.

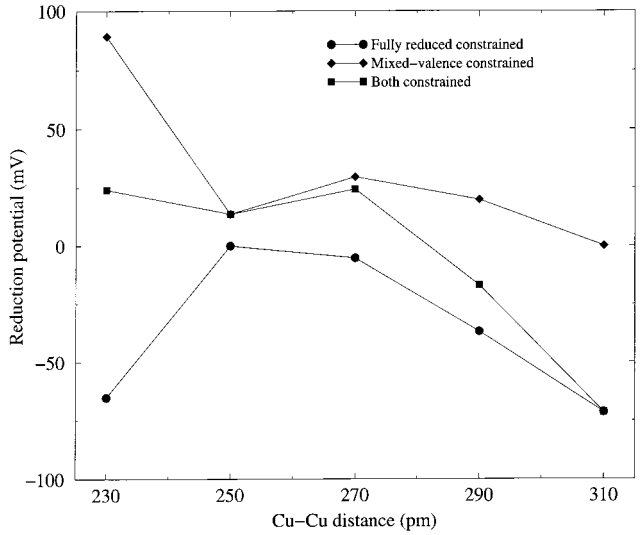

Figure 6. Calculated reduction potential for the Cu_A model between the mixed-valence and the fully reduced states as a function of constraints in the Cu−Cu bond length, calculated in water solution. The energy scale has been selected so that the unconstrained case has a reduction potential of 0 mV for all curves.

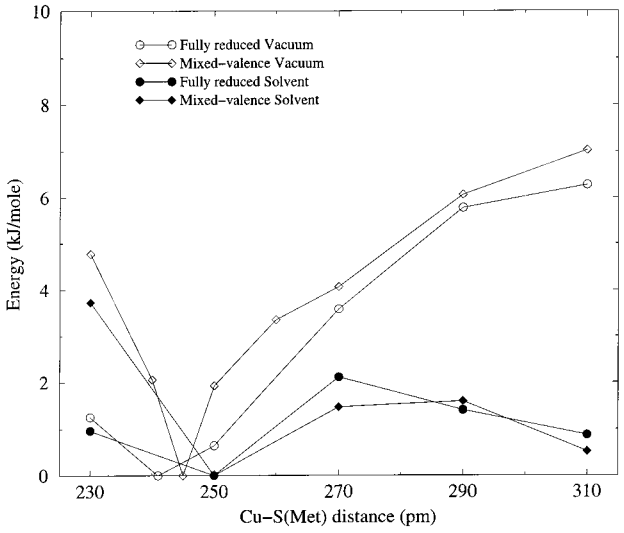

Figure 7. Potential energy surface of the $Cu-S_{Met}$ interaction in a vacuum and water for the σ^* mixed-valence and the fully reduced states of the Cu_A model.

0.13 *e*). In the reduced state, the Cu−Cu overlap population is unaltered (0.06 *e*), whereas the other overlaps are larger (0.23−0.33 and 0.12−0.15 *e*, respectively). In the π state, the Cu−Cu overlap is much smaller, less than 0.002 *e*. An examination of the electron density between the various bonds in the complex gave similar results. Thus, the Cu−Cu interaction is appreciably weaker than the weak bonds to the axial ligands.

In the mixed-valence state of the binuclear Cu_A site, the singly occupied orbital is perpendicular to the axial ligand, that is, in the CuS_2Cu plane. Therefore, it is unlikely that the axial ligands in the binuclear Cu_A site would bind more tightly than in the blue copper proteins. For the latter proteins, we have shown that the $Cu-S_{Met}$ and Cu−O potential surfaces are extremely flat and have a very limited influence on the reduction potential of the copper site.[42,45] Therefore, it is not surprising that the potential energy surfaces of these two bonds are also very flat in the Cu_A site, both in the fully reduced and the mixed-valence state, as can be seen in Figures 7 and 8. The two bond lengths can vary over a range of nearly 100 pm at an energy cost of

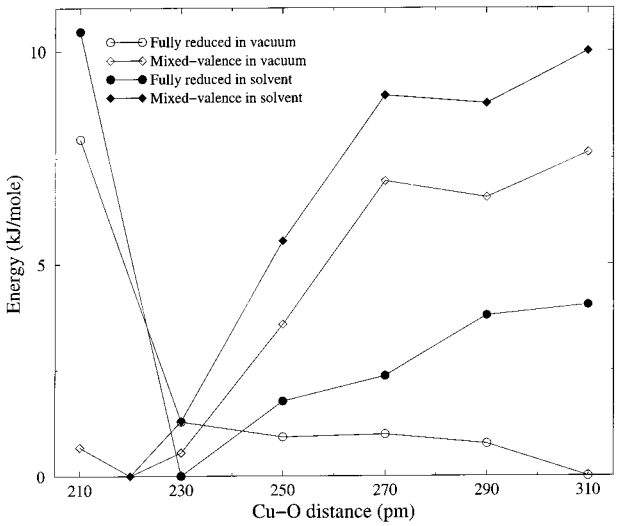

Figure 8. Potential energy surface of the Cu−O interaction in a vacuum and water for the σ^* mixed-valence and the fully reduced states of the Cu_A model.

less than 8 kJ/mol, in a vacuum as well as in water solution. This explains the large variation observed in crystal structures of cytochrome *c* oxidase (cf. Table 1). With such flexible potentials, the bond length in the protein is determined more by interactions with the surrounding protein than by the interaction with the metal ion. In particular, it is unlikely that the protein can change the structure of the Cu_A site by varying the $Cu-S_{Met}$ or Cu−O distances, as has been suggested.[8,17]

A few features in the two figures are notable. In most cases, the solvent does not change the energies much. However, for the $Cu-S_{Met}$ potential at larger distances, the vacuum energy increases for both oxidation states, whereas the potential for the reduced complex in water solution decreases. Moreover, the Cu−O vacuum curve in the reduced state is most remarkable. Apparently, this bond length can vary from 230 to 310 pm at the expense of 1 kJ/mol. Thus, this bond length is not determined by the Cu−O interaction at all.

The optimum distance for the carbonyl ligand in the mixed-valence state is short, 220 pm. At first, this may seem strange, considering that the Cu−O bond in azurin is around 310 pm.[71] In fact, it has been suggested that the shortest Cu−O distances observed in crystal structures of cytochrome *c* oxidase (down to 219 pm) are erroneous.[7] However, considering that the backbone amide group is chemically not very different from the side-chain amide group of glutamine, and that the latter group binds at a short distance in stellacyanin (around 220 pm),[71] it is not very surprising that a similar distance can be observed for Cu_A. In fact, the optimum vacuum distance for the Cu−O interaction is short (∼220 pm) both for stellacyanin and azurin models.[45,72] This has been thoroughly studied for native and Co-substituted azurin (which has a short Co−O distance also in the crystal structure.[45]

As discussed above, it has been suggested that the protein determines the structure and reduction potential of the Cu_A site by varying the distances of the axial ligands to the copper ions.[8,17] Therefore, we show in Figures 9 and 10 the reduction potential of the Cu_A models as a function of the constrained $Cu-S_{Met}$ and Cu−O distances. Curves are shown only for the water case; those in a vacuum are closely similar and can be

(71) Gray, H. B.; Malmström, B. G.; Williams, R. P. J. *J. Biol. Inorg. Chem.* **2000**, *5*, 551.
(72) De Kerpel, J. O. A.; Pierloot, K.; Ryde, U.; Roos, B. O. *J. Phys. Chem. B* **1998**, *102*, 4638.

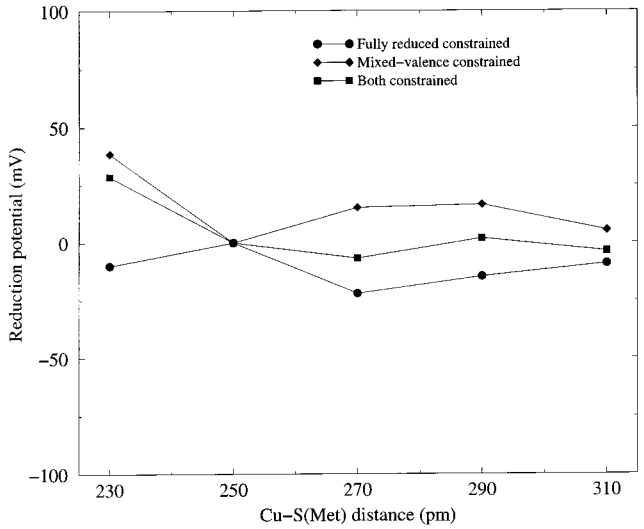

Figure 9. Calculated reduction potential for the Cu_A model between the σ^* mixed-valence and the fully reduced states as a function of constraints in the $Cu-S_{Met}$ bond length, calculated in water solution. The energy scale has been selected so that the unconstrained case has a reduction potential of 0 mV for all curves.

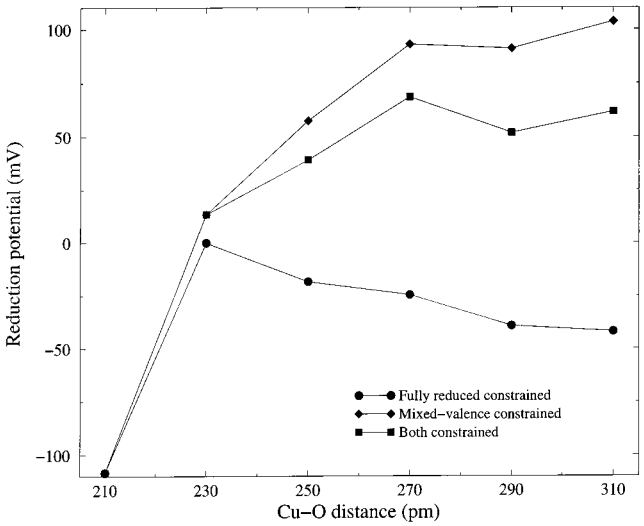

Figure 10. Calculated reduction potential for the Cu_A model between the σ^* mixed-valence and the fully reduced states as a function of constraints in the Cu−O bond length, calculated in water solution. The energy scale has been selected so that the unconstrained case has a reduction potential of 0 mV for all curves.

quite easily deduced from the results in Figures 7 and 8. The curves clearly show that these distances have a small influence on the reduction potential of the Cu_A site. Variations in the $Cu-S_{Met}$ bond between 230 and 310 pm can change the reduction potential by at most 60 mV, whereas variations in the Cu−O bond between 210 and 310 pm can have slightly larger effects, up to 100 mV. These changes are only a small part of the difference between model complexes and the Cu_A in the protein, −280 mV compared to around +250 mV[8]. Instead, this difference is most likely caused by the differing dielectric properties. For example, the reduction potential of a heme group ligated to an octapeptide is 300−500 mV lower than that in a protein, and synthetic [4Fe−4S] clusters have reduction potentials that are 500−800 mV lower than those in ferredoxins.[73]

Strain in the Protein or in Model Complexes? It has been argued that the strain-less state of Cu_A should be similar to the

(73) Zhou, H.-X. *J. Biol. Inorg. Chem.* **1997**, *2*, 109.

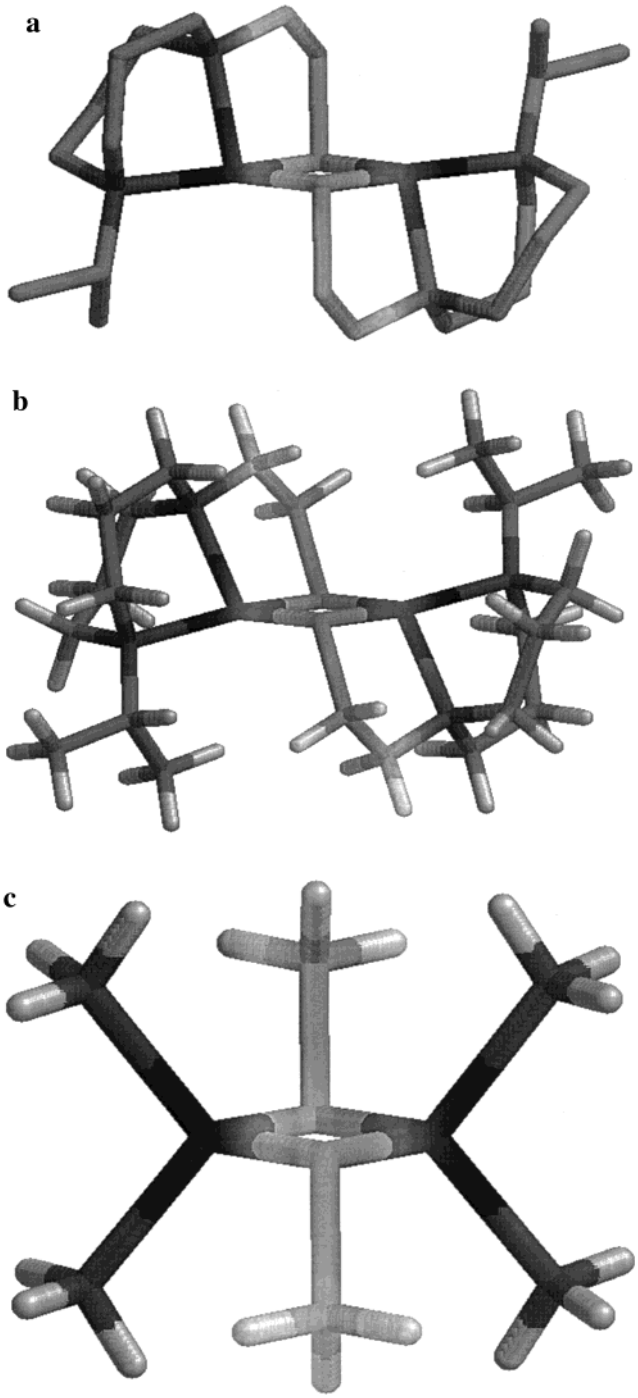

Figure 11. Crystal structure of the mixed-valence Tolman complex[34] (a), and two optimized models of it: (b) $Cu_2S_2N_4C_{22}H_{46}^+$ in the π state and (c) $((NH_3)_2Cu(SCH_3))_2^+$ in the σ^* state.

mixed-valence inorganic model prepared by Tolman and coworkers[34] (shown in Figure 11a), and that a modulation of the strength of the axial ligands by protein strain may change the electronic state of the complex to the one found in the protein.[8,17] This is in conflict with our results, which indicate that a variation in the strength of axial interactions may only have a very limited influence on the structure or reduction potential. The reason for this discrepancy is probably that the model complex is a quite poor model of the site in the protein. For example, the histidine ligands are modeled by amine groups, which are expected to bind appreciably more weakly to copper than imidazole ligands. Moreover, the axial ligands (carbonyl and thioether groups in the Cu_A site) are also modeled by the same

Table 5. Geometry and Stability (in kJ/mol) of Some Optimized Structures with Relation to the Cu_A Model Synthesized by Tolman and Co-workers[a]

model system	Cu−Cu	Cu−S	Cu−N	S−Cu−S	relative energy
$Cu_2S_2N_4C_{22}H_{46}^+$, π	304	228−237	217−221	99	0.0
$Cu_2S_2N_4C_{22}H_{46}^+$,constrained	248[b]	231	221−229	115	25.3
$Cu_2S_2N_4C_{22}H_{46}^+$,constrained	258[b]	235−240	212−226	115	17.5
$((N(CH_3)_3)_2Cu(SCH_3))_2^+$, π	319	233	225−226	94	0.0
$((N(CH_3)_3)_2Cu(SCH_3))_2^+$, σ	226	233	226−227	110	8.3
$((NH_3)_2Cu(SCH_3))_2^+$, π	309	230−233	215−217	96	0.0
$((NH_3)_2Cu(SCH_3))_2^+$, σ*	248	233	215	115	1.0
$(Im)(S(CH_3)_2)Cu(SCH_3)_2Cu(Im)(CH_3CONHCH_3)$, π	310	227−236	203−210	95−97	0.0
$(Im)(S(CH_3)_2)Cu(SCH_3)_2Cu(Im)(CH_3CONHCH_3)$, σ*	248	231−235	202−209	114−116	1.6
X-ray[34]	290−293	223−230	209−213	100	

[a] The two electronic states of our Cu_A model is also included for comparison. All structures are studied in the mixed-valence state. [b] This bond length was kept fixed during the geometry optimisation.

type of amine ligands. Finally, all of the ligand atoms are connected by covalent carbon links which may induce severe strain in the complex.

To check this suggestion, we have optimized the structure of the full Tolman complex ($Cu_2S_2N_4C_{22}H_{46}^+$) using the same methods as for the Cu_A models. The result is shown in Figure 11b and is described in Table 5. It can be seen that the crystal structure is reasonably well reproduced; the general structure of the two complexes is very similar but the average Cu−Cu, Cu−S, and Cu−N bonds are, respectively, 12, 5, and 7 pm too long in the optimized structure. This is caused by deficiencies in the B3LYP method,[40,44] in combination with a shallow Cu−Cu potential and the absence of crystal interactions in the calculation. The optimized structure is also quite similar to the π structure of the Cu_A model. Thus, both have a long Cu−Cu bond 304−310 pm, nearly identical Cu−S bond lengths and S−Cu−S angles (99° compared to 95−97°). The geometry is much less similar to the σ* Cu_A model, which has a shorter Cu−Cu bond (248 pm) and wider S−Cu−S angles (114−116°). Thus, the electronic structure of the model complex is clearly closer to the π than to the σ* state of Cu_A.

As expected, the Cu−N distances are 7−15 pm longer in the Tolman model than in the two Cu_A models, confirming that the amine groups are appreciably weaker ligands than imidazole. The amine group seems to be a reasonable model of the carbonyl ligand in Cu_A, because both bind at a distance of ∼220 pm, whereas it is a poor model of the methionine ligand, binding more than 20 pm too close. Apparently, the ligands in the model strongly stabilize the π electronic state. We have not been able to find a stable structure with a short Cu−Cu and a σ* electronic state; at a Cu−Cu distance of 248 pm (the optimum distance in our Cu_A model), the structure is destabilized by 25 kJ/mol (18 kJ/mol at 258 pm, allowing for the error in the calculated Cu−Cu distance) and more than 3 times more if the complex is constrained to C_i symmetry as in the crystal.

It is conceivable that some of the differences between the model complex and Cu_A are also caused by strain in the macrocyclic connections between the ligands in the model. Therefore, we have optimized a small model without these links, $((NH_3)_2Cu(SCH_3))_2^+$. As can be seen in Table 5, the results for the π state of this model are quite similar to those of the full model, with similar bond lengths and angles around the copper ions. However, for this small model, a stable σ* state could also be found, with an optimum Cu−Cu distance of 248 pm (Figure 11c). Most interestingly, this state is only 1 kJ/mol higher in energy than the π state.

To confirm this observation, we also optimized an intermediate complex, $((N(CH_3)_3)_2Cu(SCH_3))_2^+$, where most of the carbon atoms in the links are present, but they are not connected. The chemical properties of the amine groups in this model can be expected to be more similar to those of the model complex. Satisfactorily, this complex is intermediate both in structure and energy: The π state is most stable, and it has a Cu−Cu bond length of 309 pm. However, there is also a stable σ* state with a Cu−Cu bond length of 266 pm. It is only 8 kJ/mol less stable than the π state. Both complexes show clear effects of crowding by the methyl groups, leading to an increase in all bond lengths.

Thus, the destabilization of the σ* state in the full model complex is caused by the connections between the ligands. In Figure 11c it can be seen that in the stable σ* states, the four amine groups are placed symmetrically above and below the CuS_2Cu plane. There, they can interact with one lobe of the singly occupied Cu 3d orbital, stabilizing the complex. This is confirmed by a significant spin density on all four nitrogens (0.02 *e*). However, in the full model complex (Figure 11b shows the optimum π state, but the structure constrained to a Cu−Cu distance of 248 pm has the same general geometry), the macrocyclic connections force two amine groups almost into the CuS_2Cu plane, whereas the other two are far from the plane. This strongly favors the π structure, where the amine group in the CuS_2Cu plane can overlap with the singly occupied Cu 3d orbital, whereas the other shows a very small overlap. Therefore, the spin density of the in-plane nitrogens (0.06 *e*) is about 10 times larger than that of the out-of-plane nitrogens.

In conclusion, this shows that the difference between the protein and the model complex actually is caused by strain. However, not strain in the protein but in the model. Intuitively, this is not too unexpected. In a protein, groups interact by hydrogen bonds, van der Waals contacts, and dihedral torsions. These interactions are weak—of the same strength or weaker than the metal−ligand bonds. However, in the model complex, strain is enforced by covalent bonds in the macrocycle. Such bonds are appreciably stronger than the metal−ligand bonds, which therefore can be forced to distort.[74] Thus, a model complex is not necessarily unstrained only because it is small. This illustrates the danger of drawing too strong conclusions from inorganic models, especially if the model ligands differ from those in the protein.

The Fully Oxidized State. Finally, we have also optimized the structure of the fully oxidized state ($Cu^{II}+Cu^{II}$), which has not been observed yet. As can be seen in Table 1, the optimum structure of the fully oxidized site has a long Cu−Cu distance (342 pm) and rather short $Cu-S_{Cys}$ distances (228−234 pm). Moreover, Figure 12 shows that the ligand arrangement around the copper ions is more tetragonal than in the other states.

(74) Ryde, U. In *Recent Research Developments in Protein Engineering*; Pandalai, S. G., Ed.; Research Signpost: Trivandrum, 2001, in press.

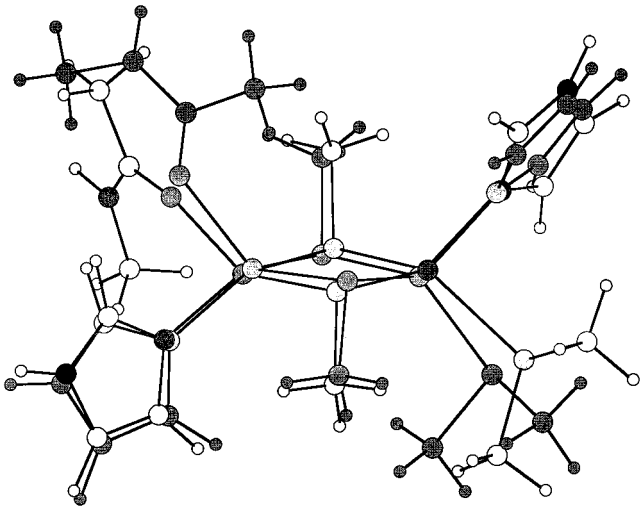

Figure 12. Structure of fully oxidized state of the Cu_A model compared to the π-bonded mixed-valence structure (shaded).

However, it is far from square-planar, the preferred geometry for Cu^{II} ions. The optimized structure is similar to another (fully oxidized) inorganic model studied by Tolman and co-workers;[33] apart from that, the copper ions are five-coordinate with three amine nitrogen ligands each in the model (cf. Table 1). In particular, the angles in the CuS_2Cu core are very similar, 85 and 92° for the S−Cu−S and Cu−S−Cu angles, respectively, compared to 83 and 92° in the model.

The fully oxidized state has a structure quite different from that of the σ^* mixed-valence state. Therefore, it is not surprising that the corresponding reorganization energy (133 kJ/mol) is four times as large as that between the mixed-valence σ^* state and the fully reduced state (43 kJ/mol, see Table 3). This is mainly an effect of λ_{ox}, which is almost twice as large as λ_{red}. It can be rationalized by examining the Cu−Cu potential energy surface for the fully oxidized state, which increases steeply at short Cu−Cu distances and shows that the $[(Cu^I+Cu^I)/(Cu^I+Cu^{II})]$ redox couple is more appropriate for electron transfer than the $[(Cu^I+Cu^{II})/(Cu^{II}+Cu^{II})]$ couple. The mixed-valence π state, however, has a Cu−Cu distance more similar to the fully oxidized state. Therefore, the reorganization energy is lower, 90 kJ/mol, but still not as low as for the native reaction of the Cu_A site.

Conclusions

In this paper, we have studied the structural and electron-transfer properties of the Cu_A dimer in its three oxidation states. We have shown that the structure is not strained to any significant degree (<10 kJ/mol), that is, not more than metal sites in other proteins (all proteins slightly distort a bound metal coordination sphere because the surrounding protein is different from vacuum or water).[74,75] Instead, the mixed-valence model compound prepared by Tolman and co-workers,[34] which has been supposed to represent a strainless Cu_A site,[8] is strained by the macrocyclic connections between the ligand models (by at least 18 kJ/mol).

Moreover, we have shown that it is unlikely that a variation in the strength of axial interactions may change the structure or reduction potential of the site significantly, contrary to what has been suggested before.[8,17] This latter suggestion was based on the large variation of the bond lengths to the axial ligands observed in crystal structures. As discussed above, this variation is caused by the flexibility of these bonds.

This investigation has also shown that the properties of the Cu_A dimer are very similar to those of the blue copper proteins. Each copper ion has a trigonal structure with a weakly bound axial ligand in the same way as in the blue-copper site. Moreover, both sites involve two nearly degenerate electronic states in the oxidized form. For the blue copper proteins, the structure may be trigonal and π-bonded (with respect to the $Cu-S_{Cys}$ bond), as in the axial type 1 protein, or tetragonal and σ-bonded, as in the rhombic type 1 proteins.[76,77] The energy of these two structures is the same within 7 kJ/mol. For Cu_A, the two electronic states for the mixed-valence complex are also very close in energy. In both cases, this degeneration gives a site with a high plasticity and a reduced inner-sphere reorganization energy.

Similarly, the axial ligands of the two sites bind to the copper ions with extremely flexible bonds. Again, this lowers the reorganization energy of the site. Another mechanism to reduce the reorganization energy of the sites is the delocalization of the charge of the copper ions onto the sulfur atoms. This reduces the actual charge on the copper ion, so that it attains properties similar to Cu(I), for example a trigonal or tetrahedral coordination geometry. In the Cu_A site, the reorganization energy is further reduced by delocalization of the unpaired electron over the four atoms in the mixed-valence state. Thus, the antibonding orbital is spread over four bonds instead of being localized to one as in the blue copper proteins. This reduces the geometry change of the oxidized form even more.[30,67]

This investigation has illustrated the strength of theoretical methods for the study of metal sites in proteins. It is *energies* that determine the rate and direction of chemical processes. Energies are the prime product in theoretical calculations, but they are often hard to measure experimentally. Therefore, indirect information is often used to get clues about the energies. We have seen that this is not always straightforward. It may be tempting to believe that a large variation in a bond length implies an important function. However, without the corresponding force constant, such a conclusion is weak. Instead, a small change in a stiff bond may be the most important factor. Unfortunately, such a variation is not discernible at the present accuracy of crystal structures. Thus, during the last years, theoretical calculations have become an important complement to experiments for the investigation of the structure and function of metal proteins.

Acknowledgment. This investigation has been supported by grants from the Swedish Natural Science Research Council (NFR) and by computer resources of the Swedish Council for High Performance Computing (HPDR), Parallelldatorcentrum (PDC) at the Royal Institute of Technology, Stockholm, and Lunarc at Lund university.

Supporting Information Available: Tables 6−12, coordinates and energies for the optimized complexes (PDF). This material is available free of charge via the Internet at http://pubs.acs.org.

JA010315U

(75) Ryde, U.; Olsson, M. H. M.; Roos, B. O.; De Kerpel, J. O. A.; Pierloot, K. *J. Biol. Inorg. Chem.* **2000**, *5*, 565.

(76) Olsson, M. H. M.; Ryde, U.; Roos, B. O.; Pierloot, K. *J. Biol. Inorg. Chem.* **1998**, *3*, 109.

(77) Pierloot, K.; De Kerpel, J. O. A.; Ryde, U.; Olsson, M. H. M.; Roos, B. O. *J. Am. Chem. Soc.* **1998**, *120*, 13156.